

# First-Principles Investigation of Energetics and Electronic Structures of Ni and Sc Co-Doped MgH<sub>2</sub>

Gaili Sun<sup>1,2</sup>, Yuanyuan Li<sup>1</sup>, Xinxin Zhao<sup>2</sup>, Yiming Mi<sup>1,2\*</sup>, Lili Wang<sup>2\*</sup>

<sup>1</sup>College of Chemistry and Chemical Engineering, Shanghai University of Engineering Science, Shanghai, China

<sup>2</sup>College of Fundamental Studies, Shanghai University of Engineering Science, Shanghai, China

Email: \*yimingmi@sues.edu.cn, \*llwang@sues.edu.cn

Received 10 December 2015; accepted 18 January 2016; published 22 January 2016

Copyright © 2016 by authors and Scientific Research Publishing Inc.

This work is licensed under the Creative Commons Attribution International License (CC BY).

<http://creativecommons.org/licenses/by/4.0/>



Open Access

---

## Abstract

First-principles calculations were used to study the energetics and electronic structures of Ni and Sc co-doped MgH<sub>2</sub> system. The preferential positions for dopants were determined by the minimal total electronic energy. The results of formation enthalpy indicate that Ni and Sc co-doped MgH<sub>2</sub> system is more stable than Ni single-doped system. The hydrogen desorption enthalpies of these two hydrides are investigated. Ni and Sc co-doping can improve the dehydrogenation properties of MgH<sub>2</sub>. The lowest hydrogen desorption enthalpy of 0.30 eV appears in co-doped system, which is significantly lower than that of Ni doping. The electronic structure analysis illustrates that the hybridization of dopants with Mg and H atom together weakens the Mg-H interaction. And the Mg-H bonds are more susceptible to dissociate by Ni and Sc co-doping because of the reduced magnitude of Mg-H hybridization peaks. These behaviors effectively improve the dehydrogenation properties of Ni and Sc co-doped cases.

## Keywords

First-Principles Calculation, MgH<sub>2</sub>, Stability, Enthalpy, Dehydrogenation Property, Electronic Structure

---

## 1. Introduction

Hydrogen energy with high efficiency and pollution-free characteristics [1]-[5], is considered to be one of the most promising candidates to replace fossil fuels. The safe and cost-effective hydrogen storage methods are

\*Corresponding authors.

some of the key factors for its practical applications [2]. It is desirable for the hydrogen “container” to have high gravimetric capacities, store and transport hydrogen economically and conveniently [3]-[5]. Storing hydrogen chemically in solid hydrides with atomic state has the potential to fulfill these requirements. Among solid hydrides, magnesium hydride ( $\text{MgH}_2$ ) has been investigated extensively in the last two decades due to its high hydrogen storage capacity (7.6 wt%), good cyclability, cheap cost and lightweight of magnesium [5]-[7]. Unfortunately, a high thermodynamic stability and poor kinetics in the reaction of hydrogenation and dehydrogenation hampered practical applications of  $\text{MgH}_2$  [6]-[8].

Over the past several decades, many efforts have been made to overcome these disadvantages. Reducing the grain size [7]-[9], and introducing transition metals (TM) or transition metals oxides [10]-[14], can effectively improve the absorption/desorption kinetics of  $\text{MgH}_2$ . Among these two methods, the introduction of transition metals into  $\text{MgH}_2$  has played a vital role in the development of Mg-based hydrogen storage materials. The thermodynamic properties and dehydrogenation kinetics of  $\text{MgH}_2$  can be tuned by doping it with different TM [10] [14]. Larsson *et al.* [14] carried out first-principles calculations based on DFT which showed that Ti, V, Fe, and Ni significantly lowered the  $\text{H}_2$  desorption energies of  $\text{MgH}_2$  nanoclusters and improved these dehydrogenation properties. Pozzo *et al.* [15] observed that Ni is the best possible choice of the transition metal doped on Mg(0001) surfaces due to low activation barriers for hydrogen dissociation and diffusion processes. More recently, many researchers reported that the hydrogen desorption kinetics of  $\text{MgH}_2$  can further be tuned by multi-doping it with different TM [16]-[22]. A computational study carried out by Huang *et al.* [17] showed that the capacity retaining rate of  $\text{Mg}_{1.5}\text{Ti}_{0.5}\text{Ni}$  milled alloys is better than that of  $\text{Mg}_2\text{Ni}$  milled alloys. Zhang and the co-workers [16] found that the combined effect of Al and Ni weakens the Mg-Ni and Ni-H interactions and decreases bonding electrons number below Fermi level. Zhou *et al.* [20] showed that co-doping Y and Al in  $\text{MgH}_2$  can weaken Mg-H bonds and promote the desorption of hydrogen. Despite the many experimental and theoretical studies of co-doped  $\text{MgH}_2$  hydrogen storage system, there is still a lack of systematic study of the structural, bonding and hydrogen desorption properties of co-doped  $\text{MgH}_2$  with Ni and Sc.

Thus in this paper, we conducted a systematic study on the effects of Ni and Sc co-doped on  $\text{MgH}_2$  using first-principles calculations. We have studied the preferential sites of Ni and Sc dopants on  $\text{MgH}_2$  depending on the minimization of total electronic energy. The dopants' influence on structural stability and dehydrogenation properties of the  $\text{MgH}_2$  were investigated by formation enthalpies and hydrogen desorption enthalpies. Electronic structures were analyzed to identify the intrinsic mechanisms of interactions between Mg and dopants and the desorption of hydrogen on co-doped system.

## 2. Computational Model and Method

$\text{MgH}_2$  has a rutile type tetragonal structure (P42/mnm, group No.136) with experimentally measured lattice parameters of  $a = 4.501 \text{ \AA}$  and  $c = 3.010 \text{ \AA}$  [23]. In the unit cell of  $\text{MgH}_2$ , two Mg atoms occupy the  $2a$  (0, 0, 0) site and four H atoms occupy the  $4f$  (0.303, 0.303, 0) site. Previously, we calculated the lattice parameters of  $\text{MgH}_2$  are  $a = 4.477 \text{ \AA}$  and  $c = 2.989 \text{ \AA}$ , these results are in full agreement with experimental and other theoretical values [12] [20]. For Ni and Sc co-doped on  $\text{MgH}_2$  system, we simulate a  $3 \times 3 \times 1$  supercell model (see **Figure 1**) that contained a total of 54 atoms with four non-equivalent positions for Mg and six non-equivalent positions for H. The  $\text{MgH}_2$   $3 \times 3 \times 1$  supercell is computed using the bulk parameters. Relaxations of the atomic coordinates were carried out, the optimal atomic positions of Mg and H atoms are good agreement with other theoretical data [20].

All energy and electronic structure calculations were performed under the framework of the density functional theory (DFT) via the Vienna *ab initio* Simulation Package (VASP) [24]. The electron-ion core interactions were described by the projector augmented wave (PAW) method [25]. The Perdew-Wang 91 (PW91) functional as generalized gradient approximation (GGA) was adopted for the exchange-correlation term [26]. For the plane-wave basis set a cutoff energy of 350 eV was used. A Gaussian smearing method for geometry optimization and a tetrahedron method with Blöchl corrections for electronic structures with an energy broadening of 0.05 eV were used throughout. Dependence of total energy on k-mesh was checked, a  $3 \times 3 \times 7$  Monkhorst-Pack k-point mesh for geometry optimization and a  $5 \times 5 \times 9$  Monkhorst-Pack k-point mesh for electronic structures were used to save the computing cost. The total energy convergence was chosen to be  $10^{-7}$  eV and the absolute magnitude of force on each atom was below 0.01 eV/Å.

### 3. Results and Discussion

#### 3.1. Dopant Site Preference and Substitution Energy

In order to find the optimum geometry and doped sites of dopants (Ni and Sc) in  $\text{MgH}_2$ , the total electronic energies of dopants in every non-equivalent position need to be calculated. In the Ni-doped system, each of the four non-equivalent positions of Mg is substituted by Ni in order. The calculated total electronic energies are shown in **Figure 2(a)**. Due to the minimal total electronic energy, Ni prefers to substitute for the Mg3 position, and the new compound is denoted as  $(\text{Mg}, \text{Ni})\text{H}_2$ . Then, Mg is substituted by Sc in other three non-equivalent positions (Mg1, Mg2 and Mg4) of  $(\text{Mg}, \text{Ni})\text{H}_2$  compound. The calculated total electronic energies are shown in **Figure 2(b)**. It can be seen that Sc prefers to substitute for the Mg4 position due to its lowest total electronic energy, and the new compound is denoted as  $(\text{Mg}, \text{Ni}, \text{Sc})\text{H}_2$ . Hence, in co-doped system, the Mg3 and Mg4 would be simultaneously substituted by Ni and Sc, respectively.

To identify the favorability of Ni and Y co-doping in  $\text{MgH}_2$  comparing to Ni single-doping, the substitution energies ( $E_{\text{sub}}$ ) of  $(\text{Mg}, \text{Ni})\text{H}_2$  and  $(\text{Mg}, \text{Ni}, \text{Sc})\text{H}_2$  are estimated via the definition [21] [27]:

$$E_{\text{sub}} = 1/54 \left[ E_t(\text{Mg}_{18-x-y}\text{Ni}_x\text{Sc}_y\text{H}_{36}) - E_t(\text{Mg}_{18}\text{H}_{36}) - xE_b(\text{Ni}) - yE_b(\text{Sc}) + (x+y)E_b(\text{Mg}) \right] \quad (1)$$

where  $E_t(M)$  refer to the total energies of supercell of hydrides.  $E_b$  represents the total energies per atom in the bulk structure. The  $x$  and  $y$  are the number of dopants in the supercell. The obtained substitution energies of  $(\text{Mg}, \text{Ni})\text{H}_2$  and  $(\text{Mg}, \text{Ni}, \text{Sc})\text{H}_2$  are 0.16 and 0.12 eV/atom, respectively. From energy point of view, the smaller substitution energy corresponds to the more favorable substitution doping. Therefore, the co-doping Ni and Sc into  $\text{MgH}_2$  is most energetically favorable than the single-doping Ni into  $\text{MgH}_2$ .

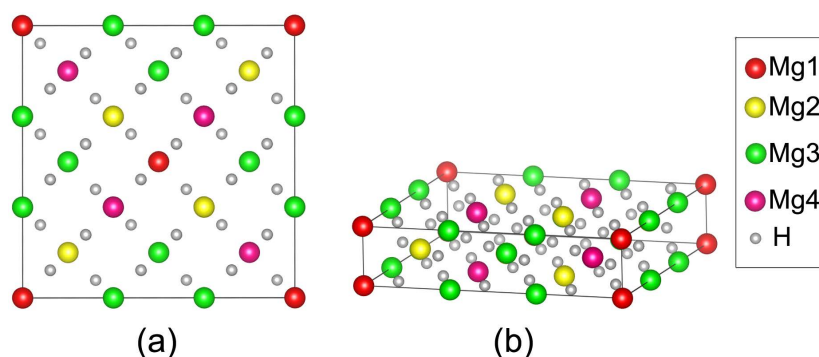


**Figure 1.** Top (a) and side (b) views of  $\text{MgH}_2$   $3 \times 3 \times 1$  supercell model. Mg1, Mg2, Mg3 and Mg4 denote four non-equivalent position for Mg, respectively.

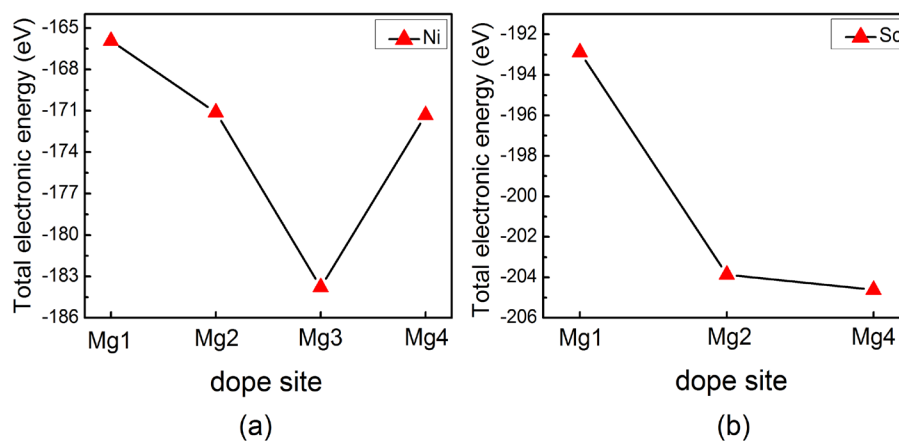


**Figure 2.** The total electronic energy of (a) doped  $\text{Mg}_{18}\text{H}_{36}$  with Ni in four non-equivalent positions of Mg; (b) doped  $(\text{Mg}, \text{Ni})\text{H}_2$  with Sc in the other non-equivalent positions of Mg.

### 3.2. Stability and Dehydrogenation Properties

In general, the structural stability of crystal is closely related to the formation enthalpy ( $\Delta H_{\text{form}}$ ), negative formation enthalpy indicates that the crystal can exist stably. Furthermore, the more negative formation enthalpy suggests the higher stability of crystal [28]. The formation enthalpy ( $\Delta H_{\text{form}}$ ) is calculated in order to recognize the stability of the co-doped system compared to single-doped system, using the follow definition [28] [29]:

$$\Delta H_{\text{form}} = 1/54 \left[ E_t(\text{Mg}_{18-x-y}\text{Ni}_x\text{Sc}_y\text{H}_{36}) - xE_b(\text{Ni}) - yE_b(\text{Sc}) - (18-x-y)E_b(\text{Mg}) - 18E(\text{H}_2) \right] \quad (2)$$

where  $E_t$  represents the total energies of supercell of hydrides.  $E_b$  is the total energies per atom in the bulk structure. The  $x$  and  $y$  are the number of dopants in the supercell.  $E(\text{H}_2)$  denotes the total energy of free  $\text{H}_2$  molecule is computed as  $-6.77$  eV, which was evaluated via a  $8 \times 8 \times 8 \text{ \AA}$  supercell in full agreement with experimental [5] and other theoretical data [12] [18]. The calculated formation enthalpies of  $(\text{Mg}, \text{Ni})\text{H}_2$  and  $(\text{Mg}, \text{Ni}, \text{Sc})\text{H}_2$  are  $-0.06$  and  $-0.10$  eV/atom, respectively. It can be seen that the formation enthalpies of these two compounds are both negative, which means that these compounds can exist stably. Besides, Ni and Sc co-doped system has lower enthalpy value, which means co-doped system exhibits higher stability compared to Ni single-doping.

In order to further assess the dehydrogenation abilities of  $(\text{Mg}, \text{Ni})\text{H}_2$  and  $(\text{Mg}, \text{Ni}, \text{Sc})\text{H}_2$ , their hydrogen desorption enthalpies ( $\Delta H_{\text{des}}$ ) are also calculated by using Equation (3) [5] [30]:

$$\Delta H_{\text{des}} = 1/n \left[ E_t(\text{Mg}_{18-x-y}\text{Ni}_x\text{Sc}_y\text{H}_{36-2n}) + nE(\text{H}_2) - E_t(\text{Mg}_{18-x-y}\text{Ni}_x\text{Sc}_y\text{H}_{36}) \right] \quad (3)$$

where  $E_t(\text{Mg}_{18-x-y}\text{Ni}_x\text{Sc}_y\text{H}_{36})$  represents the total energy of supercell of hydrides.  $E_t(\text{Mg}_{18-x-y}\text{Ni}_x\text{Sc}_y\text{H}_{36-2n})$  refers to a pseudostructure in which  $2n$  H atoms are removed from the relaxed  $\text{Mg}_{18-x-y}\text{Ni}_x\text{Sc}_y\text{H}_{36}$  system.  $E(\text{H}_2)$  is the same as that used in Equation (2). In the dehydrogenation process,  $n$  is equivalent to 2 for move out H1, H2 and H3 atom with the  $\text{Mg}_{18-x-y}\text{Ni}_x\text{Sc}_y\text{H}_{36-2n}$  compound and  $n$  is equivalent to 4 for move out H4, H5 and H6 atom with the  $\text{Mg}_{18-x-y}\text{Ni}_x\text{Sc}_y\text{H}_{36-2n}$  compound.

For the Ni single-doped  $\text{MgH}_2$  system, the hydrogen desorption enthalpies are shown in **Figure 3(a)**. The corresponding  $\Delta H_{\text{des}}$  values are 1.86, 1.67, 1.72, 0.52, 1.02 and 0.57 eV/ $\text{H}_2$  for H1 - H6 respectively. Compare with the hydrogen desorption enthalpy of  $\Delta H_{\text{des}} = 0.77$  eV/ $\text{H}_2$  results for  $\text{MgH}_2$  in 570 K [16], part desorption enthalpies of Ni-doped  $\text{MgH}_2$  are decreased. Therefore, the H (H4, H6) around dopant Ni would be released easily, due to the smaller hydrogen desorption enthalpy. For the Ni and Sc co-doped  $\text{MgH}_2$  system, the hydrogen desorption enthalpies of Ni and Sc co-doped are shown in **Figure 3(b)**. The corresponding  $\Delta H_{\text{des}}$  values are 0.75, 1.35, 0.67, 0.34, 1.09 and 0.30 eV/ $\text{H}_2$  for H1 - H6, respectively. It can be observed that most of the hydrogen desorption enthalpies for this hydride are significantly decreased in comparison with Ni doping, except for the  $\Delta H_{\text{des}}$  value of H5 around Mg. Thus most hydrogen dissociation is much easier than single-doped case, which indicates the Ni and Sc co-doped system has more promising dehydrogenation properties. Although the partial substitution of Mg by Ni and Sc has significant effects on  $\text{MgH}_2$ , the detailed understanding of the effect of co-doping of Ni and Sc on the hydrogen desorption process and kinetics of  $\text{MgH}_2$  requires a further investigated, which will be the subject of our future work.

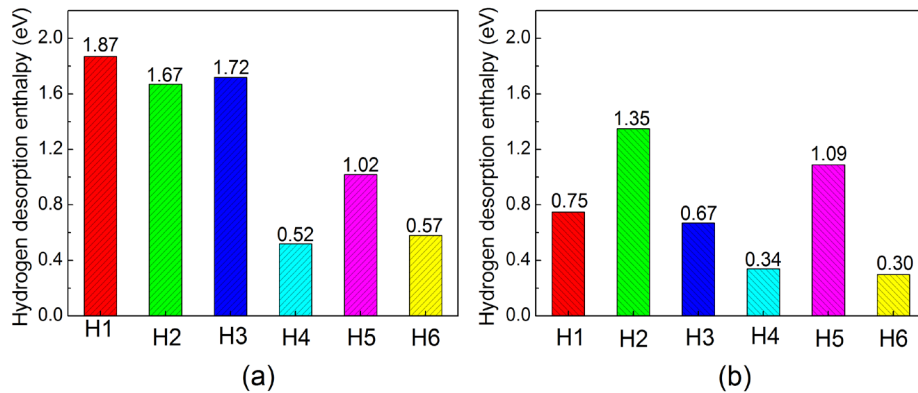


**Figure 3.** The calculated hydrogen desorption enthalpies by moving out H atoms (H1 - H6) for (a)  $(\text{Mg}, \text{Ni})\text{H}_2$ ; (b)  $(\text{Mg}, \text{Ni}, \text{Sc})\text{H}_2$ .

### 3.2. Geometrical Feature and Bonding Interactions

**Table 1** presents the bond distances between metallic elements of undoped and doped MgH<sub>2</sub> systems. The bond length of Mg-Mg range from 3.500 Å to 4.476 Å with an average of 3.663 Å in pure MgH<sub>2</sub> system, which is in good agreement with other theoretical results [20] [31]. In Ni single-doped MgH<sub>2</sub> system, Mg2 and Mg4 are the nearest neighboring metallic atoms of the dopant Ni. The average of Mg-Ni bond length is 3.692 Å, shorter than that of Mg-Mg bond in pure MgH<sub>2</sub>, which implies the bond strength of Mg-Ni is enhanced. The bond length of Mg-Mg is also decreased, thus the strength of Mg-Mg bond is enhanced in comparison with that of the pure MgH<sub>2</sub>. For Ni and Sc co-doped system, the bond length of Mg-Mg is further decreased, enhancing the strength of Mg-Mg bond. The distances between the Mg and Ni atoms are longer than that of the single-doped system, indicates that its bond strength are weakened. Furthermore, the length of Mg2-Sc bond and the Ni-Sc bond are shorter than the Ni-doped system, thus the bond strength of Mg2-Sc and Ni-Sc are enhanced. These can be inferred that the dopant Sc has alloying trend with Mg and Ni atoms, which would be weakened the strength of Mg-H and Ni-H bonds.

**Table 2** lists the interaction of metallic and H atoms of doped MgH<sub>2</sub>. In this calculation, the bond length of Mg-H ranges from 1.926 Å to 1.941 Å with an average of 1.934 Å, consistent with the experimental [29] and other theoretical results [32] [33]. For the MgH<sub>2</sub> single-doped with Ni, H4, H5 and H6 atoms are the nearest neighboring atoms of dopant Ni and these atoms move towards Ni, thus the bond length of Mg-H (H4 - H6) are increased. Compared with undoped MgH<sub>2</sub>, the bond lengths of Mg-H5 and Mg-H6 are increased with 0.008 Å and 0.304 Å, respectively. Therefore, the bond strength of Mg-H is weakened by Ni doping. For the MgH<sub>2</sub> co-doped with Ni and Sc, the bond length of Ni-H (H4, H6) is longer than that of Ni single-doped system, thus the strength of Mg-H (H4, H6) bond is weakened. H2, H3 and H5 atoms are the nearest neighboring atoms of the dopant Sc and the length of Sc-H is increased compared with Mg4-H bond, and then the strength of Sc-H bond is weakened. Comparing with Ni single-doped system, the bond length of Ni-H (H4, H6) and Mg-H (H2, H6) are increased, so the dopant Sc can further weaken the Mg-H and Ni-H bond.

### 3.3. Electronic Structure

The total and partial density of states (DOS) of the pure MgH<sub>2</sub> system are plotted in **Figure 4**, the Fermi energy

**Table 1.** Calculated the bond distance (Å) between metallic elements in the hydrides.

MgH <sub>2</sub>	Mg1-Mg2	Mg1-Mg3	Mg1-Mg4	Mg2-Mg3	Mg2-Mg4	Mg3-Mg4
	3.501	4.476	3.501	3.500	3.500	3.500
(Mg, Ni)H <sub>2</sub>	Mg1-Mg2	Mg1-Ni	Mg1-Mg4	Mg2-Ni	Mg2-Mg4	Ni-Mg4
	3.272	4.322	3.269	3.445	3.203	3.300
(Mg, Ni, Sc)H <sub>2</sub>	Mg1-Mg2	Mg1-Ni	Mg1-Sc	Mg2-Ni	Mg2-Sc	Ni-Sc
	3.208	4.350	3.381	3.684	3.170	3.106

**Table 2.** Calculated the bond distance (Å) between H and metallic atoms in the hydrides.

(Mg, Ni)H <sub>2</sub>	Mg1-H1	1.789	Mg2-H1	1.833	Ni-H4(1)	1.760	Mg4-H2	1.781
	Mg1-H2	1.836	Mg2-H3	1.800	Ni-H4(2)	1.623	Mg4-H3	1.765
			Mg2-H6	2.238	Ni-H5	1.656	Mg4-H5	1.942
(Mg, Ni, Sc)H <sub>2</sub>					Ni-H6	1.683		
	Mg1-H1	1.746	Mg2-H1	1.826	Ni-H4(1)	1.780	Sc-H2	1.913
	Mg1-H2	1.842	Mg2-H3	1.749	Ni-H4(2)	1.669	Sc-H3	1.835
			Mg2-H6	2.544	Ni-H5	1.639	Sc-H5	1.970
				Ni-H6	1.735			

( $E_F$ ) level is set at zero and used as a reference. The energy gap between the valence band (VB) and conduction band (CB) is 3.82 eV. The value is in good agreement with other theoretical calculations reported previously [20] [34]. The relatively large energy gap of  $MgH_2$  leads to a high formation enthalpy and poor hydrogen sorption kinetics of  $MgH_2$  [35]. The DOSs plot corresponding to  $MgH_2$  shows a large dispersion of the bands signaling the s-like character. The VB is mainly dominated by H s orbitals and the CB mainly by Mg s and Mg p orbitals. The amplitude of the partial DOS of the H s orbital is a result of the weight of H in the structure, and also of the transfer of electronics from Mg to H leading to an ionic hydride.

The total and partial DOS of Ni-doped  $MgH_2$  system are plotted in Figure 5. The amplitude of the partial DOS of the Ni d orbital was minimized by 10 in order to plot the partial DOSs of all atoms in the same panel with the same scale. The total DOS curve shows a remarkable decrease in the band gap of 0 eV, show clearly metallic characteristics. Ni doping leads to the appearance of a narrow d-band in the middle of the band gap.

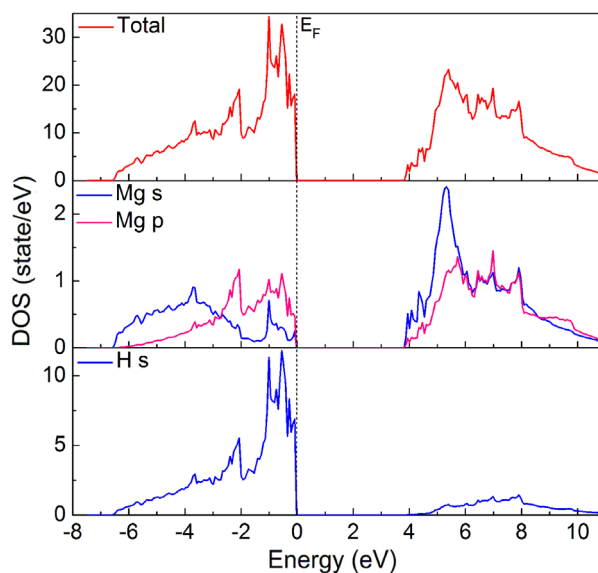


**Figure 4.** Total and partial electronic densities of states of the pure  $MgH_2$ .

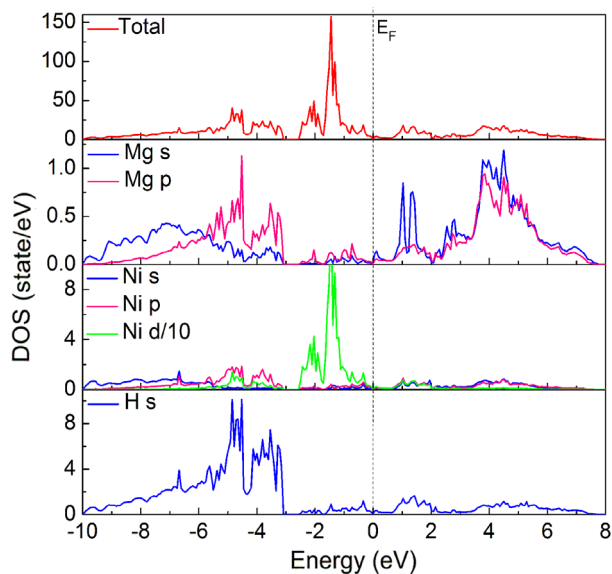


**Figure 5.** Total and partial electronic densities of states of Ni single-doped  $MgH_2$  system.

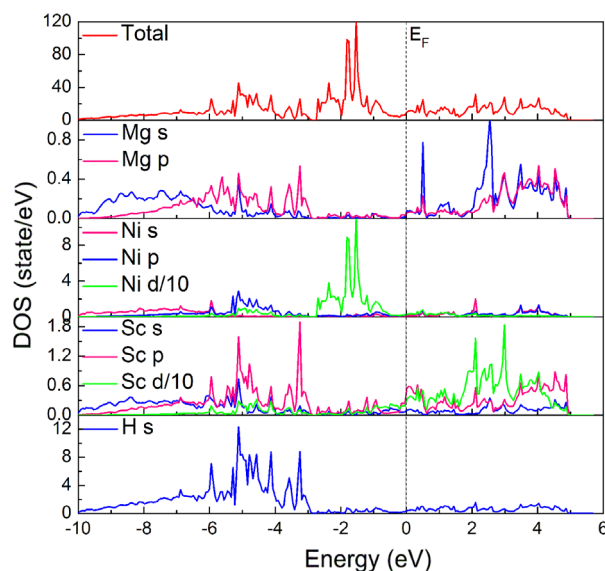


**Figure 6.** Total and partial electronic densities of states of Ni and Sc co-doped  $\text{MgH}_2$ .

This d orbital is strongly hybridized with Mg p and H s orbitals giving the strongly Mg-Ni and Ni-H bonding. Furthermore, the H s orbitals distributed in the region of  $-5.5$  to  $-3.1$  eV are less overlapped with Mg s p orbitals comparing to pure  $\text{MgH}_2$ , and the amplitude of the valence band is decreased, which can help to weaken the hybridization of Mg-H bond. These weak bonding interactions between Mg and H in Ni doped system are the reasons why this system has better dehydrogenation property.

The total and partial DOS of the Ni and Sc co-doped  $\text{MgH}_2$  system are plotted in **Figure 6**. Similar to the Ni single-doped system, the amplitude of the partial DOS of the Ni and Sc d orbitals were minimized by 10 in order to plot the partial DOSs of all atoms in the same panel with the same scale. The similar lowered bonding peaks of H s, Mg s and p orbitals can also be observed, indicating the Mg-H bond is further weakened after Sc doping. The Sc p and d orbitals overlap with H s, Mg p, Ni p and d orbitals in the energy region of  $-3.2$  to  $6.1$  eV. And the distributions of bonding peaks of Sc d orbitals are mainly concentrated in the energy region of  $1.8$  to  $4.2$  eV and overlap well with Mg s and p orbitals. These behaviors indicate that Sc atom has strong bonding interaction with H, Mg and Ni atoms and decreases Mg-H p-s mixing. Therefore, the Mg-H hybridizations are significantly weakened in Ni and Sc co-doped system, and this system exhibits more promising dehydrogenation property.

#### 4. Conclusion

In summary, the Ni and Sc co-doping effects on the energetics and electronic structures of  $\text{MgH}_2$  were studied by the first-principles calculations based on DFT. Due to the minimal total electronic energy, Ni and M dopants prefer to substitute the Mg3 and Mg4 positions, respectively. The substitution energy and formation enthalpy are used to estimate the energetic stability of the doped  $\text{MgH}_2$  system. Ni and Sc co-doped  $\text{MgH}_2$  system are more stable than Ni single-doped system. The hydrogen desorption enthalpies of these three systems were also studied. According to the relatively lower hydrogen desorption enthalpies, the co-doped systems possess more promising dehydrogenation properties compared with pure Ni doping. And the lowest hydrogen desorption enthalpy of  $0.30$  eV appears in co-doped system. The electronic structure analysis illustrates that the hybridization of dopants with Mg and H atom together weakens the Mg-H interaction. The decrease in hybridization peaks of Mg-H and band gaps leads to an easier Mg-H dissociation and lower hydrogen desorption enthalpy when the  $\text{MgH}_2$  is co-doped with Ni and Sc. Therefore, the co-doping with Ni and Sc effectively improves the dehydrogenation properties of destabilized  $\text{MgH}_2$ .

#### Acknowledgements

The work was supported by the National Natural Science Fund (No. 11504228) and the Graduated Innovative

Research Project of Shanghai University of Engineering Science (No. E1-0903-14-01107-14KY0411) and the Innovation Program of Shanghai Municipal Education Commission, China (10YZ172).

## References

- [1] Züttel, A. (2003) Materials for Hydrogen Storage. *Mater Today*, **6**, 24-33. [http://dx.doi.org/10.1016/S1369-7021\(03\)00922-2](http://dx.doi.org/10.1016/S1369-7021(03)00922-2)
- [2] Schlapbach, L. and Züttel, A. (2001) Hydrogen-Storage Materials for Mobile Applications. *Nature*, **414**, 353-358. <http://dx.doi.org/10.1038/35104634>
- [3] Hao, S.Q. and Sholl, D.S. (2012) Effect of TiH<sub>2</sub> Induced Strain on Thermodynamics of Hydrogen Release from MgH<sub>2</sub>. *Journal of Physical Chemistry C*, **116**, 2045-2050. <http://dx.doi.org/10.1021/jp210573a>
- [4] Tang, J.J., Yang, X.B., Chen, L.J. and Zhao, Y.J. (2014) Modeling and Stabilities of Mg/MgH<sub>2</sub> Interfaces: A First-Principles Investigation. *AIP Advances*, **4**, Article ID: 077101. <http://dx.doi.org/10.1063/1.4886384>
- [5] Dai, J.H., Song, Y. and Yang, R. (2010) First Principles Study on Hydrogen Desorption from a Metal (= Al, Ti, Mn, Ni) Doped MgH<sub>2</sub> (110) Surface. *Journal of Physical Chemistry C*, **114**, 11328-11334. <http://dx.doi.org/10.1021/jp103066g>
- [6] Tang, J.J., Yang, X.B., Chen, M., Zhu, M. and Hao, Y.J. (2012) First-Principles Study of Biaxial Strain Effect on Hydrogen Adsorbed Mg (0001) Surface. *Journal of Physical Chemistry C*, **116**, 14943-14949. <http://dx.doi.org/10.1021/jp303480c>
- [7] Mina, Y., Hanno, H.W. and Zhang, Z.Y. (2011) First-Principles Studies of Hydrogen Interaction with Ultrathin Mg and Mg-Based Alloy Films. *Physical Review B*, **83**, 045413. <http://dx.doi.org/10.1103/PhysRevB.83.045413>
- [8] Callini, E., Pasquini, L., Jensen, T.R. and Bonetti, E. (2013) Hydrogen Storage Properties of Mg-Ni Nanoparticles. *International Journal of Hydrogen Energy*, **38**, 12207-12212. <http://dx.doi.org/10.1016/j.ijhydene.2013.05.139>
- [9] Johansson, M., Ostenfeld, C.W. and Chorkendorff, I. (2006) Adsorption of Hydrogen on Clean and Modified Manganese Films. *Physical Review B*, **74**, 193408. <http://dx.doi.org/10.1103/PhysRevB.74.193408>
- [10] Chen, M., Yang, X.B., Cui, J., Tang, J.J., Gan, L.Y., Zhou, M. and Zhao, Y.J. (2012) Stability of Transition Metals on Mg(0001) Surfaces and Their Effects on Hydrogen Adsorption. *International Journal of Hydrogen Energy*, **37**, 309-317. <http://dx.doi.org/10.1016/j.ijhydene.2011.09.065>
- [11] Zhang, J., Zhou, D.W., Peng, P. and Liu, J.S. (2008) First-Principles Investigation of Mg<sub>2</sub>TH<sub>y</sub> (T = Ni, Co, Fe) Complex Hydrides. *Physica B*, **403**, 4217-4223. <http://dx.doi.org/10.1016/j.physb.2008.09.009>
- [12] Germán, E., Verdinelli, V., Luna, C.R., Juan, A. and Sholl, D. (2014) A Theoretical Study of the Effect of Zr-, Nb-Doped and Vacancy-Like Defects on H Desorption on MgH<sub>2</sub> (110) Surface. *Journal of Physical Chemistry C*, **118**, 4231-4237. <http://dx.doi.org/10.1021/jp411714d>
- [13] Mamula, B.P., Novaković, J.G., Radisavljević, I., Ivanović, N. and Novaković, N. (2014) Electronic Structure and Charge Distribution Topology of MgH<sub>2</sub> Doped with 3d Transition Metals. *International Journal of Hydrogen Energy*, **39**, 5874-5887. <http://dx.doi.org/10.1016/j.ijhydene.2014.01.172>
- [14] Larsson, P., Araujo, C.M., Larsson, J.A., Jena, P. and Ahuja, R. (2008) Role of Catalysts in Dehydrogenation of MgH<sub>2</sub> Nanoclusters. *Proceedings of the National Academy of Sciences of the United States of America*, **105**, 8227-8231. <http://dx.doi.org/10.1073/pnas.0711743105>
- [15] Pozzo, M. and Alfè, D. (2009) Hydrogen Dissociation and Diffusion on Transition Metal (=Ti, Zr, V, Fe, Ru, Co, Rh, Ni, Pd, Cu, Ag)-Doped Mg(0001) Surfaces. *International Journal of Hydrogen Energy*, **34**, 1992-1930. <http://dx.doi.org/10.1016/j.ijhydene.2008.11.109>
- [16] Zhang, J., Huang, Y.N., Peng, P., Mao, C., Shao, Y.M. and Zhou, D.W. (2011) First-Principles Study on the Dehydrogenation Properties and Mechanism of Al-Doped Mg<sub>2</sub>NiH<sub>4</sub>. *International Journal of Hydrogen Energy*, **36**, 5375-5382. <http://dx.doi.org/10.1016/j.ijhydene.2011.02.002>
- [17] Huang, L.W., Elkedim, O., Nowak, M., Chassagnon, R. and Jurczyk, M. (2012) Mg<sub>2-x</sub>Ti<sub>x</sub>Ni (x = 0, 0.5) Alloys Prepared by Mechanical Alloying for Electrochemical Hydrogen Storage: Experiments and First-Principles Calculations. *International Journal of Hydrogen Energy*, **37**, 14248-14256. <http://dx.doi.org/10.1016/j.ijhydene.2012.07.036>
- [18] Zhang, J., Huang, Y.N., Mao, C., Peng, P., Shao, Y.M. and Zhou, D.W. (2011) Ab Initio Calculations on Energetics and Electronic Structures of Cubic Mg<sub>3</sub>MNi<sub>2</sub> (M = Al, Ti, Mn) Hydrogen Storage Alloys. *International Journal of Hydrogen Energy*, **36**, 14477-14483. <http://dx.doi.org/10.1016/j.ijhydene.2011.08.016>
- [19] Gutfleisch, O., Dal, T.S., Herrich, M., Handstein, A. and Pratt, A. (2005) Hydrogen Sorption Properties of Mg-1 wt.% Ni-0.2 wt.% Pd Prepared by Reactive Milling. *Journal of Alloys and Compounds*, **404**, 413-416. <http://dx.doi.org/10.1016/j.ijhydene.2011.08.016>
- [20] Zhou, S.C., Pan, R.K., Luo, T.P., Wu, D.H., Wei, L.T. and Tang, B.Y. (2014) Ab Initio Study of Effects of Al and Y Co-Doping on Destabilizing of MgH<sub>2</sub>. *International Journal of Hydrogen Energy*, **39**, 9254-9261.



- <http://dx.doi.org/10.1016/j.ijhydene.2014.04.007>
- [21] Song, Y., Zhang, W.C. and Yang, R. (2009) Stability and Bonding Mechanism of Ternary (Mg, Fe, Ni)H<sub>2</sub> Hydrides from First Principles Calculations. *International Journal of Hydrogen Energy*, **34**, 1389-1398. <http://dx.doi.org/10.1016/j.ijhydene.2008.11.046>
- [22] Kalinichenka, S., Rontzsch, L. and Kieback, B. (2009) Structural and Hydrogen Storage Properties of Melt-Spun Mg-Ni-Y Alloys. *International Journal of Hydrogen Energy*, **34**, 7749-7755. <http://dx.doi.org/10.1016/j.ijhydene.2009.07.053>
- [23] Ono, S., Ishido, Y., Imanari, K., Tabata, T., Cho, Y. and Yamamoto, R. (1982) Phase Transformation and Thermal Expansion of MgNi Alloys in a Hydrogen Atmosphere. *Journal of the Less Common Metals*, **88**, 57-61. [http://dx.doi.org/10.1016/0022-5088\(82\)90014-5](http://dx.doi.org/10.1016/0022-5088(82)90014-5)
- [24] Kresse, G. and Furthmüller, J. (1996) Efficient Iterative Schemes for *Ab initio* Total-Energy Calculations Using a Plane-Wave Basis Set. *Physical Review B*, **54**, 11169-11187. <http://dx.doi.org/10.1103/PhysRevB.54.11169>
- [25] Blöchl, P.E. (1994) Projector Augmented-Wave Method. *Physical Review B*, **50**, 17953-17979. <http://dx.doi.org/10.1103/PhysRevB.50.17953>
- [26] Perdew, J.P. and Wang, Y. (1992) Accurate and Simple Analytic Representation of the Electron-Gas Correlation Energy. *Physical Review B*, **45**, 13244-13249. <http://dx.doi.org/10.1103/PhysRevB.45.13244>
- [27] Song, Y., Guo, Z.X. and Yang, R. (2004) Influence of Selected Alloying Elements on the Stability of Magnesium Dihydride for Hydrogen Storage Applications: A First-Principles Investigation. *Physical Review B*, **69**, Article ID: 094205. <http://dx.doi.org/10.1103/PhysRevB.69.094205>
- [28] Fischer, T. and Almlof, J. (1992) General Methods for Geometry and Wave Function Optimization. *Journal of Physical Chemistry C*, **96**, 9768-9774. <http://dx.doi.org/10.1021/j100203a036>
- [29] Tang, B.Y., Wang, N., Yu, W.Y., Zeng, X.Q. and Ding, W.J. (2008) Theoretical Investigation of Typical Fcc Precipitates in Mg-Based Alloys. *Acta Materialia*, **279**, 192-200. <http://dx.doi.org/10.1016/j.actamat.2008.03.014>
- [30] Zhang, J., Huang, Y.N., Mao, C. and Peng, P. (2012) Synergistic Effect of Ti and F Co-Doping on Dehydrogenation Properties of MgH<sub>2</sub> from First-Principles Calculations. *Journal of Alloys and Compounds*, **538**, 205-211. <http://dx.doi.org/10.1016/j.jallcom.2012.05.098>
- [31] Bortz, M., Berthel, B., Böttger, G. and Yvon, K. (1999) Structure of the High Pressure Phase  $\gamma$ -MgH<sub>2</sub> by Neutron Powder Diffraction. *Journal of Alloys and Compounds*, **287**, L4-L6. [http://dx.doi.org/10.1016/S0925-8388\(99\)00028-6](http://dx.doi.org/10.1016/S0925-8388(99)00028-6)
- [32] Jain, I.P., Lal, C. and Jain, A. (2010) Hydrogen Storage in Mg: A Most Promising Material. *International Journal of Hydrogen Energy*, **35**, 5133-5144. <http://dx.doi.org/10.1016/j.ijhydene.2009.08.088>
- [33] Shi, B. and Song, Y. (2013) Influence of Transition Metals Fe, Ni and Nb on Dehydrogenation Characteristics of Mg(BH<sub>4</sub>)<sub>2</sub>: Electronic Structure Mechanisms. *International Journal of Hydrogen Energy*, **38**, 6417-6424. <http://dx.doi.org/10.1016/j.ijhydene.2013.03.061>
- [34] Yu, R. and Lam, P.K. (1988) Electronic and Structural Properties of MgH<sub>2</sub>. *Physical Review B*, **37**, 8730-8737. <http://dx.doi.org/10.1103/PhysRevB.37.8730>
- [35] Zeng, X.Q., Cheng, L.F., Zou, J.X., Ding, W.J., Tian, H.Y. and Buckley, C. (2012) Influence of 3d Transition Metals on the Stability and Electronic Structure of MgH<sub>2</sub>. *Journal of Applied Physics*, **111**, Article ID: 093720. <http://dx.doi.org/10.1063/1.4714549>